

# RADIATIVE CORRECTIONS TO $\tau$ PAIR PRODUCTION AROUND $Z_0^*$

BY Z. WĄS

Institute of Nuclear Physics, Cracow\*\*

(Received November 12, 1986)

It is studied to what extent the QED bremsstrahlung effects may obscure the experimental verification of the standard electroweak theory by means of measuring quantities/distributions related to  $\tau$  spin polarization in the  $\tau$  production process around the  $Z_0$  resonance. In the presented investigation the following effects are taken into account: single hard bremsstrahlung from  $e^\pm$  and  $\tau^\pm$ , leading one loop corrections of the standard theory, longitudinal spin polarization of  $e^\pm$  and the spin polarization effects in  $\tau^+\tau^-$  decays. All numerical results are obtained using a Monte Carlo event generator for the combined  $\tau^\pm$  production and decay process. It is shown that the radiative effects are definitely less sizable on the top of  $Z_0$  than off the peak. They depend strongly on kinematical cut-offs used to eliminate the hard bremsstrahlung effects. Also a number of analytical calculations are presented, notably a new simple parametrization of the hard bremsstrahlung spin amplitudes.

PACS numbers: 12.15.Ii

## 1. Introduction

The last two decades brought up a new picture of fundamental interactions of elementary particles. Standard Model based on the gauge group  $SU(3) \times SU(2) \times U(1)$  and three families of leptons and quarks seems to agree rather well with a wide range of the presently available experimental data.

Even though Standard Model is renormalizable and anomaly free, presence of about 20 free parameters in the basic theory is a strong indication of our incomplete insight in the underlying dynamics.

The QCD sector of the Standard Model agrees rather well with experiment, although it is plagued with problems due to confinement and weakly convergent perturbative expansion.

On the other hand, electro-weak interactions as described by the Glashow-Salam-Weinberg model [1] are free of these difficulties and theoretical predictions can be obtained

---

\* Work supported in part by the grants CPBP 01.09 I.2.2.0.01 and CPBP 01.03 2.4.

\*\* Address: Instytut Fizyki Jądrowej, Zakład V, Kawory 26a, 30-055 Kraków, Poland.

in principle, with high precision. The QED sector of the Standard Model is confirmed by experiment with high precision and over a wide range of energies and processes. In particular, QED radiative corrections are in spectacular agreement with experiment.

Situation in the remaining non QED part of the GSW model is different. Even its basic assumptions, like universality of coupling constants in the fermionic sector and gauge nature of intermediate heavy bosons are rather far from being fully confirmed by experiment.

The  $e^+e^-$  scattering experiments of SLC and LEP [2, 3] will open a new field for precise tests of the GSW model in a more complete form.

Due to complexity of the modern high energy experiments, to presence of multi-particle final state phase space, and to complicated structure of cut-offs used to define observables, it is often not enough to present theoretical predictions in a form of formulae or tables. A definitely better method of representing theoretical predictions is to implement them in a form of the Monte Carlo event generator. Then, the influence of all apparatus effects and cut-offs on the measured observables can be brought under control much more easily.

Background problems, often present in the data analysis, are also more efficiently handled using a packet of the M. C. programs. Typically, a M. C. event generator used to analyze data for one process is also used to estimate background for another process.

In this paper I will concentrate on the combined process of production and decay of  $\tau$ -pairs in the  $Z_0$  region. A unique property of this reaction is that the spin polarization of the final state  $\tau$ -lepton can be measured using its decay products (without any additional investment in the detector). This measurement will play a role of the important data point for the precise tests of the Standard Model, almost as important as  $Z_0$  mass or muon forward/backward asymmetry.

In practice, the polarization measurement, as other quantities measured in  $e^+e^-$  scattering, will be a subject to familiar problems, which are due to a complicated interrelation of the experimental cut-offs with the QED bremsstrahlung effects. Fortunately these effects are calculable and, in the data analysis, may be accounted for with arbitrary precision. To this end one needs a good M. C. event generator simulating  $\tau$  pair production and decay, which includes QED hard bremsstrahlung and other QED/GSW radiative corrections. The M. C. programs of this type will be indispensable in the precise comparisons of the GSW model with the experimental data in LEP/SLC experiments.

Since the ultimate precision goal for many measurements in LEP/SLC experiments is 1% or even less (one expects to measure  $Z_0$  mass and width with accuracy up to 10–20 MeV Muon forward/backward asymmetry with accuracy of 0.002 and  $\tau$  polarization with accuracy of 0.015 [4]), therefore one should envisage 0.1% accuracy level as a desired target for the M.C. program dedicated for  $\tau$  production and decay process. This means that terms of order  $(\alpha/\pi \ln(S/m_e^2))^2$ ,  $\alpha/\pi \ln(S/m_e^2)$  and  $\alpha/\pi$  should be kept in the calculations. Terms like  $m_e^2/S$  for  $S \sim M^2$  may be safely neglected.

The goal of this paper is twofold. First it collects spin amplitudes and related formulae needed for the next Monte Carlo program [5] of the ultimate precision 0.1%. On the other hand, it also presents some numerical results obtained using the intermediate Monte

Carlo program, based on the modified muon Monte Carlo program of Ref. [7], which serves to estimate effects of radiative corrections in SLC/LEP1 energy range with accuracy of about 1 %. More precisely it takes care of all effects of order  $\alpha/\pi \ln(S/m_e^2)$  and of many effects of order  $\alpha/\pi$ , in a complete GSW model, including hard QED bremsstrahlung.

## 2. Spin amplitudes and photon spectra

It is known [8, 9] that spin amplitudes are very useful in numerical calculations of differential cross-sections especially in the case of processes with spin effects and/or for processes with a large number of Feynman graphs.

Spin amplitudes are shorter and easier to control. They will certainly be used to facilitate many calculations in the order  $O(\alpha^4)$  QED processes; like double bremsstrahlung [10], or multifermion final states [9]. The above methods, based on spin amplitudes, are especially efficient when combined with the M.C. integration over the phase space.

The reasons for great simplifications resulting from the use of spin amplitudes, as compared with classical method based on calculating analytically contributions to the differential cross-section prior to numerical evaluation, are rather simple. Typically number of terms in an analytical expression for the differential cross-section is roughly proportional to the square of number of Feynman graphs (note that there are 8 graphs for the reaction  $e^+e^- \rightarrow \tau^+\tau^-$  and 108 for the reaction  $e^+e^- \rightarrow e^+e^-e^+e^-$ ), while typically a number of terms in spin amplitudes grows linearly with the number of graphs.

Analytical formulae for the differential cross-section also become longer when one allows for many polarized particles (both in the initial and final state). In the Monte Carlo calculations combined with methods based on spin amplitudes this problem can be solved by the numerical contraction of spin amplitudes with density matrices or decay distributions [11].

In this Section I shall present spin amplitudes for the process  $e^+e^- \rightarrow \tau^+\tau^-(\gamma)$  in a form suitable for the precise ( $\sim 0.1\%$ ) M.C. calculations around  $Z_0$  peak.

Contributions from different QED gauge invariant groups of graphs are separated. The amplitudes are expressed using a set of independent variables which nicely parametrize spin amplitudes, and which may also be used to parametrize in a natural way two or three particle final state phase space. This parametrization will also be useful in constructing an efficient Monte Carlo algorithm.

Spin amplitudes and phase space are normalized as in [13]. The formulae are in a form ready for the extensive fast and exact numerical evaluation. In particular our formulae do not contain numerically large contributions which cancel one another, and thus leading to machine precision problems. Phases of spin amplitudes are under control, ultraviolet singularities are removed but infrared are kept in an explicit form.

### 2.1. Phase space and notation

In this Subsection I shall present spin amplitudes for the process  $e^+e^- \rightarrow \tau^+\tau^-(\gamma)$  in the limit  $2m_\tau/\sqrt{S} \rightarrow 0$ . As in Refs [6, 7] only these terms  $O(2m_\tau/\sqrt{S})$  in the spin amplitudes are kept which give nonvanishing (in the limit  $m_\tau \rightarrow 0$ ) contribution to differential

cross-section. These amplitudes will be useful in the future calculations on the higher precision level ( $\sim 0.1\%$ ). Note that corrections of  $O(\alpha/\pi)$  which result from the collinear hard bremsstrahlung are kept under control.

In the QED cross-sections sharp peaks are present. This is the reason why parametrization of the phase space should be carefully chosen such that it suits the structure of the singularities.

I parametrize the phase space in the same way as in the older calculations for  $\tau$  pair production at lower energies [8, 11, 14, 15] (see also Fig. 1). A dominant singularity (of infrared origin) is of the type  $1/k = E/E_\gamma$  where  $E_\gamma$  is photon CMS energy and  $E = \sqrt{S}/2$  is a Center of Mass System (CMS) electron beam energy.

I divide the phase space into two parts: soft, where real photon is absent in the final

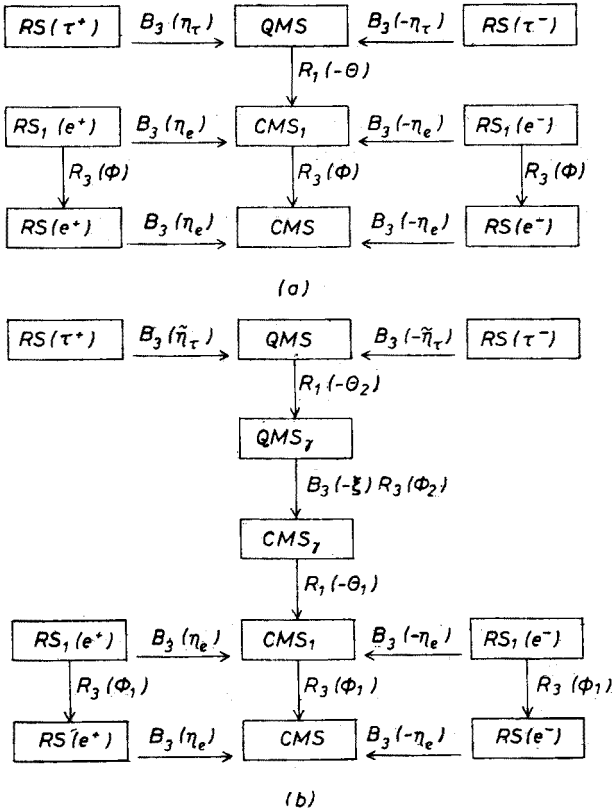


Fig. 1. Kinematics of the a)  $e^+e^- \rightarrow \tau^+\tau^-$ , b)  $e^+e^- \rightarrow \tau^+\tau^-\gamma$  processes. Boxes represent reference systems. They are connected by Lorentz transformations marked on arrows. Most important reference frames are: the Laboratory Reference system CMS, the rest system of the  $\tau^+\tau^-$  pair QMS, the rest systems of  $\tau^\pm$  leptons  $RS(\tau^\pm)$  used to quantize  $\tau^\pm$  spins and to simulate decays in the M.C. algorithm and the  $e^\pm$  rest systems  $RS(e^\pm)$  where the  $e^\pm$  polarization vectors are defined. Other intermediate systems were used for calculating spin amplitudes, to define polarization vectors of intermediate photon, etc.  $R_i(\alpha)$  denotes rotation around  $i$ -th axis by the angle  $\alpha$ .  $B_i(\xi)$  denotes boost along  $i$ -th axis with boost parameter  $\xi$ .

state or its energy is small,  $k < k_0$ , and hard, where energy of the photon in the CMS is higher than a certain threshold value,  $k > k_0$  (typically  $k_0 \sim 0.01$ ).

In CMS positron and electron four-momenta are defined as follows

$$p_1 = (E, 0, 0, E), \quad p_2 = (E, 0, 0, -E). \quad (1)$$

If real photon is absent (or soft) it is enough to introduce two angles  $\theta$  and  $\varphi$  to parametrize a two body phase space, then  $\tau^+$  and  $\tau^-$  four-momenta are defined in the CMS as follows

$$q_1 = (E, -s_\varphi s E, c_\varphi s E, c E), \quad q_2 = (E, s_\varphi s E, -c_\varphi s E, -c E). \quad (2)$$

Here the following short hand notation is used  $c = \cos(\theta)$ ,  $s = \sin(\theta)$ ,  $c_\varphi = \cos(\varphi)$ ,  $s_\varphi = \sin(\varphi)$ . The element of the two particle phase space (multiplied by the flux factor) is

$$d \text{ Lips}_2 = \frac{m_e^2 m_\tau^2}{4S\pi^2} d\Omega. \quad (3)$$

Here  $d\Omega = dcd\varphi$ ,  $m_e$  and  $m_\tau$  denote electron and  $\tau$  masses. I list also here some variables and abbreviations used later to define spin amplitudes:  $c_e = \cosh(\eta_e) = E/m_e$ ,  $c_\tau = \cosh(\eta_\tau) = E/m_\tau$ ,  $\zeta = (S - M^2)/S$ ,  $\gamma = \Gamma M/S$ .  $M$ ,  $\Gamma$  denote  $Z_0$  mass and width (on  $Z_0$  peak).

In the hard photon case, in addition to its energy  $k$ , one has to introduce four angles  $\theta_1$ ,  $\theta_2$ ,  $\varphi_1$ ,  $\varphi_2$  to parametrize the 3-body phase space. Here  $\theta_1$  denotes an angle between photon and  $e^+$  momenta in the CMS system,  $\theta_2$  denotes an angle between photon and  $\tau^+$  momenta in the QMS system (see Fig. 1). Angles  $\theta_1$ ,  $\theta_2$  parametrize in a natural way the collinear bremsstrahlung singularities of initial and final states. An angle  $\varphi_2$  is defined (up to a sign and  $\pm\pi/2$ ) as an angle between two planes, one defined by photon and  $e^+$  momenta and another defined by photon and  $\tau^+$  momenta. A  $\varphi_1$  angle, like the angle  $\varphi$  in the soft photon case, orientates a whole event around the beam axis. For exact definition of angular variables see also Fig. 1.

In the following, the other short hand notations and abbreviations will be often in use:  $c_1 = \cos(\theta_1)$ ,  $c_2 = \cos(\theta_2)$ ,  $s_1 = \sin(\theta_1)$ ,  $s_2 = \sin(\theta_2)$ ,  $c_{\varphi_1} = \cos(\varphi_1)$ ,  $c_{\varphi_2} = \cos(\varphi_2)$ ,  $s_{\varphi_1} = \sin(\varphi_1)$ ,  $s_{\varphi_2} = \sin(\varphi_2)$ . Also, the photon energy  $k$  will be sometimes replaced by a hyperbolic angle  $\xi$  related to  $k$  as follows:  $s_\xi = \sinh(\xi) = k/(2\sqrt{1-k})$ ,  $c_\xi = \cosh(\xi) = (2-k)/(2\sqrt{1-k})$ .

With these definitions the element of the three particle phase space (multiplied by the flux factor) can be written as

$$d \text{ Lips}_3 = \frac{m_e^2 m_\tau^2}{2^8 \pi^5} k dk dc_1 dc_2 d\varphi_1 d\varphi_2, \quad (4)$$

and the four-momenta of  $\tau^+$ ,  $\tau^-$  and  $\gamma$  can be parametrized in the CMS system as follows

$$q_1 = \left( \frac{2-k}{2} - \frac{k}{2} c_2, s_2 s_{\varphi_2} c_{\varphi_1} \sqrt{1-k} + \frac{k}{2} s_{\varphi_1} s_1 \right)$$

$$\begin{aligned}
& -s_{\varphi_1} c_1 s_2 c_{\varphi_2} \sqrt{1-k} - \frac{2-k}{2} s_1 c_2 s_{\varphi_1}, c_{\varphi_1} \left( -\frac{k}{2} s_1 \right. \\
& \left. + c_1 s_2 c_{\varphi_2} \sqrt{1-k} + \frac{2-k}{2} s_1 c_2 \right) + s_{\varphi_1} s_2 s_{\varphi_2} \sqrt{1-k}, \\
& -\frac{k}{2} c_1 - s_1 s_2 c_{\varphi_2} \sqrt{1-k} + \frac{2-k}{2} c_1 c_2 \Big), \\
q_2 = & \left( \frac{2-k}{2} + \frac{k}{2} c_2, -s_2 s_{\varphi_2} c_{\varphi_1} \sqrt{1-k} + \frac{k}{2} s_{\varphi_1} s_1 \right. \\
& \left. + s_{\varphi_1} c_1 s_2 c_{\varphi_2} \sqrt{1-k} + \frac{2-k}{2} s_1 c_2 s_{\varphi_1}, c_{\varphi_1} \left( -\frac{k}{2} s_1 \right. \right. \\
& \left. \left. - c_1 s_2 c_{\varphi_2} \sqrt{1-k} - \frac{2-k}{2} s_1 c_2 \right) - s_{\varphi_1} s_2 s_{\varphi_2} \sqrt{1-k}, \right. \\
& \left. -\frac{k}{2} c_1 + s_1 s_2 c_{\varphi_2} \sqrt{1-k} - \frac{2-k}{2} c_1 c_2 \right), \\
k = & (k, -k s_{\varphi_1} s_1, k c_{\varphi_1} s_1, k c_1). \tag{5}
\end{aligned}$$

I complete the parametrization of initial and final state degrees of freedom with definitions of spin states which will be used in spin amplitudes. In both the soft and the hard parts of the cross-section  $\varepsilon = \pm 1$  and  $\tau = \pm 1$  denote twice the helicities of  $e^+$  and  $\tau^+$ . The structure of spin amplitudes is more transparent if instead of taking  $e^-$  and  $\tau^-$  helicities we define variables  $\mathcal{E}$  and  $\mathcal{T}$  which say whether helicity is conserved or not (along electron or  $\tau$  fermionic lines) e.g.  $\mathcal{E} = +1$  if helicities of  $e^+$  and  $e^-$  are reverse, in opposite case  $\mathcal{E} = -1$ . Variable  $G$  denotes circular polarization of the photon.

## 2.2. Virtual photon and Born spin amplitudes

Using conventions introduced in the previous Section and definition of the coupling constants of  $Z_0$  to initial and final state fermions in a given helicity states  $g_e = v + \varepsilon a$ ,  $\tilde{g}_\tau = \tilde{v} + \tau \tilde{a}$  Born spin amplitude may be written in the following way:

$$(M_{\varepsilon\tau}^{\mathcal{E}\mathcal{T}})_{\text{BORN}} = \begin{cases} (M_{\varepsilon\tau}^{++})_{\text{BORN}} = \left( -ie^2 \frac{c_e c_\tau}{S} \right) (q\tilde{q}B_\gamma(0) + g_e \tilde{g}_\tau B_Z(0)) (\varepsilon\tau + c), \\ (M_{\varepsilon\tau}^{+-})_{\text{BORN}} = 0, \\ (M_{\varepsilon\tau}^{-+})_{\text{BORN}} = 0, \\ (M_{\varepsilon\tau}^{--})_{\text{BORN}} = 0, \end{cases} \tag{6}$$

where

$$B_\gamma(k) = \frac{1}{1-k}, \quad B_Z(k) = \frac{1}{\zeta - k + i\gamma}, \quad (7)$$

and  $q, \tilde{q}$  denote initial and final state fermions' charge in the electron charge unit. For definition of  $B_\gamma(k), B_Z(k)$  see also Section 5.

Spin amplitudes for virtual corrections of  $O(\alpha/\pi)$  are nonzero like the Born amplitude only in the case of both  $\mathcal{E}$  and  $\mathcal{T}$  being equal to  $+1$ . They may be expressed in the following way

$$\begin{aligned} M_{\epsilon\tau}^{\text{VIRT}} &= M_{\epsilon\tau}^{\text{BORN}} \left[ F_1 \left( \frac{S}{m_e^2}, \frac{m_e}{\lambda} \right) + F_1 \left( \frac{S}{m_\tau^2}, \frac{m_\tau}{\lambda} \right) \right] \\ &+ M_{\epsilon\tau}^{\text{BOX}} + \left( -ie^2 q\tilde{q} \frac{c_e c_\tau}{S} \right) (-\Pi_{\gamma\gamma}(S))(\epsilon\tau + c), \end{aligned} \quad (8)$$

$\lambda$  denotes photon mass used to regularize infrared singularities.

$$\text{Re } F_1(x, y) = \frac{\alpha}{\pi} \left[ -1 + \frac{1}{3} \pi^2 + \frac{3}{4} \ln(x) - \frac{1}{4} \ln^2(x) + (1 - \ln(x)) \ln(y) \right], \quad (9)$$

$$\Pi_{\gamma\gamma}(S) = -\frac{1}{2} \delta_{\text{vp}} \left( \frac{4m_e^2}{S} \right) - \frac{1}{2} \delta_{\text{vp}} \left( \frac{4m_\mu^2}{S} \right) - \frac{1}{2} \delta_{\text{vp}} \left( \frac{4m_\tau^2}{S} \right) + i - \frac{1}{2} \delta_{\text{had}}(S). \quad (10)$$

Here  $\delta_{\text{vp}}(z) = 2\alpha/\pi(-5/9 + 1/3 \ln(z))$  but  $\delta_{\text{had}}$  is calculated using parametrization based on substracted dispersion relations and experimental data on hadronic  $e^+e^-$  total cross-section e.g. [16, 17, 18].

Contribution from the box diagrams can be separated into two parts: two-photon boxes and  $Z_0$ -photon boxes  $M_{\epsilon\tau}^{\text{BOX}} = M_{\epsilon\tau}^{\gamma\gamma} + M_{\epsilon\tau}^{\gamma Z}$ , where

$$M_{\epsilon\tau}^{\gamma\gamma} = (q\tilde{q})^2 \left( -ie^2 \frac{c_e c_\tau}{S} \right) (\epsilon\tau Z_1 + Z_2) B_\gamma(0), \quad (11)$$

and

$$M_{\epsilon\tau}^{\gamma Z} = g_e \hat{g}_\tau q\tilde{q} \left( -ie^2 \frac{c_e c_\tau}{S} \right) (\epsilon\tau X_1 + X_2) B_Z(0), \quad (12)$$

or taking only the leading contribution proportional to the  $Z_0$  Born amplitude [6] (1% accuracy level)

$$M_{\epsilon\tau}^{\gamma Z} = g_e \tilde{g}_\tau q\tilde{q} \left( -ie^2 \frac{c_e c_\tau}{S} \right) (\epsilon\tau + c) Y B_Z(0). \quad (13)$$

In the above formulae the following functions were used:

$$Z_1 = \frac{\alpha}{2\pi} \left\{ 2 \ln \left( \frac{1-c}{1+c} \right) \left[ \ln \left( \frac{\lambda^2}{S} \right) + i\pi \right] + \ln \left( \frac{1-c}{1+c} \right) \right\}$$

$$\begin{aligned}
& -\frac{c}{1+c} \left[ \ln^2 \left( \frac{1-c}{2} \right) + i2\pi \ln \left( \frac{1-c}{2} \right) \right] \\
& -\frac{c}{1-c} \left[ \ln^2 \left( \frac{1+c}{2} \right) + i2\pi \ln \left( \frac{1+c}{2} \right) \right] \Big\}, \\
Z_2 = & \frac{\alpha}{2\pi} \left\{ 2c \ln \left( \frac{1-c}{1+c} \right) \left[ \ln \left( \frac{\lambda^2}{S} \right) + i\pi \right] + \ln \left( \frac{1-c}{2} \right) + \ln \left( \frac{1+c}{2} \right) + 2\pi i \right. \\
& -\frac{c}{1+c} \left[ \ln^2 \left( \frac{1-c}{2} \right) + i2\pi \ln \left( \frac{1-c}{2} \right) \right] \\
& \left. + \frac{c}{1-c} \left[ \ln^2 \left( \frac{1+c}{2} \right) + i2\pi \ln \left( \frac{1+c}{2} \right) \right] \right\}, \\
Y = & \frac{\alpha}{\pi} \left\{ -\ln \left( \frac{1-c}{1+c} \right) \left[ \ln \left( \frac{(M^2-S)^2 + \Gamma^2 M^2}{(M\lambda)^2} \right) - 2i \arctan \left( \frac{\Gamma M}{M^2-S} \right) \right] \right. \\
& \left. + \frac{1}{2} \ln^2 \left( \frac{1+c}{2} \right) - \frac{1}{2} \ln^2 \left( \frac{1-c}{2} \right) - \text{Li}_2 \left( \frac{1+c}{2} \right) + \text{Li}_2 \left( \frac{1-c}{2} \right) \right\}, \quad (14)
\end{aligned}$$

where the arctan function is continuous in infinity and is defined such that  $\arctan(0 \pm) = 0, \pi$ . Functions  $X_1$  and  $X_2$  can be calculated in a simple way from functions  $c^{\gamma Z}$  and  $c_s^{\gamma Z}$  of Ref. [19].  $X_1 = -(c^{\gamma Z} + cc_s^{\gamma Z})$ ,  $X_2 = -(cc^{\gamma Z} + c_s^{\gamma Z})$ . Formulae in [19] although exact are rather lengthy. Functions  $X_1, X_2$  can also be reconstructed from function  $f(s, t, u)$  of [20]. It was checked in Ref. [19], that the approximate formula for  $\gamma$ -Z box agrees numerically with the exact one quite well, provided  $S \sim M^2$ .

Virtual photon spin corrections for the pure QED part of the spin amplitudes are obtained by taking a  $m_\tau \rightarrow 0$  limit in the formulae of Ref. [8, 12]. Virtual corrections for the  $Z_0$  exchange graph were reconstructed from the cross-sections given in [6, 7]. It was once again checked analytically and in the case of  $Z_0$ -gamma boxes numerically, that in this way one obtains the same results for virtual corrections as in [19]. Imaginary part of function  $F_1$  can be found in [19], but it is irrelevant to any measurable quantity in the QED  $O(\alpha/\pi)$ .

Using notation introduced in Section 2.1 soft and virtual part of the cross-section read as follows

$$\begin{aligned}
(d\sigma_{\text{et}}^{++})_{\text{SOFT}} = & \{|M_{\text{et}}^{\text{BORN}}|^2 + 2 \text{Re}(M_{\text{et}}^{\text{VIRT}}(M_{\text{et}}^{\text{BORN}})^*)\} d\text{Lips}_2 \\
& + \left( \frac{d\sigma_{\text{et}}^{++}}{d\text{Lips}_2} \right)^{\text{SOFT PH}} d\text{Lips}_2. \quad (15)
\end{aligned}$$

Contribution from the soft photon cross-section  $(d\sigma_{\text{et}}^{++}/d\text{Lips}_2)^{\text{SOFT PH}}$  which cancels infrared singularities of virtual corrections will be defined at the end of Section 2.3.3. Photon mass plays a role of a dummy parameter and none of the final numerical results depend on it.



### 2.3. Bremsstrahlung

In the following I shall present hard bremsstrahlung spin amplitudes for  $e^+e^- \rightarrow \tau^+\tau^-\gamma$  process with  $\gamma$  and  $Z_0$  exchange in the  $S$ -channel taking  $m_\tau \rightarrow 0$  limit. The amplitudes with only  $\gamma$  exchange were obtained directly from the amplitudes of Ref. [8] by taking  $m_\tau \rightarrow 0$  limit. The amplitudes with  $Z_0$  exchange were calculated in a similar way as in Ref. [8] and the limit  $m_\tau \rightarrow 0$  was also taken. This limit was taken in such a way that most of the terms  $O(2m_\tau/\sqrt{S})$  in the spin amplitudes were dropped. Kept were only those which lead, on the level of the differential cross-section, to nonvanishing contributions of order  $O(\alpha/\pi)$ . It was checked that formulae obtained in this way reproduce the non polarized cross-sections as given in Refs [6, 7]. It was also checked that up to the overall phase these spin amplitudes coincide with the spin amplitudes of [21] (except of terms proportional to fermions' masses).

Soft bremsstrahlung contribution was taken from Refs [8, 19]. It was also calculated independently and found to agree numerically well with the approximate formulae given in [6, 7]. Photon spectrum of [6, 7] was reproduced. It was also checked that the photon spectrum of Ref. [6] (formula 3.18) referred to as approximate is in fact exact.

#### 2.3.1. Spin amplitudes

The hard bremsstrahlung spin amplitudes, calculated in the way explained above, can be written in the following way

$$\begin{aligned}
 M_{\epsilon\tau G}^{++} &= iN_h \frac{1}{2s_\tau} \left\{ q \exp(-\xi) \frac{s_1}{c_e^{-2} + s_1^2} D_{\epsilon\tau}(k) \right. \\
 &\quad \left. + \tilde{q} \exp(-iG\varphi_2) \frac{s_2}{\tilde{c}_\tau^{-2} + s_2^2} D_{\epsilon\tau}(0) \right\} K_{\epsilon\tau G}, \\
 M_{\epsilon\tau G}^{--} &= 0, \\
 M_{\epsilon\tau G}^{-+} &= \frac{1}{2} N_h \frac{\exp(-\xi)}{c_e} q \exp(iG\varphi_2) \frac{c_1}{c_e^{-2} + s_1^2} D_{-c_1\epsilon, \tau}(k) L_{\epsilon\tau G}, \\
 M_{\epsilon\tau G}^{+-} &= \frac{1}{2} N_h \frac{1}{\tilde{c}_\tau} \tilde{q} \frac{c_2}{\tilde{c}_\tau^{-2} + s_2^2} D_{\epsilon, -c_2\tau}(0) N_{\epsilon\tau G}.
 \end{aligned} \tag{16}$$

Here the following functions and definitions were used:

$$\tilde{c}_\tau = c_\tau y, \quad N_h = e^3 \frac{c_e c_\tau}{\sqrt{8} E^3}, \quad y = \exp(-\xi),$$

$$\begin{aligned}
 K_{\epsilon\tau G} &= -(\epsilon\tau + c_1 c_2) \cosh(\xi + iG\varphi_2) + s_1 s_2 \\
 &\quad - G(\tau c_1 + \epsilon c_2) \sinh(\xi + iG\varphi_2),
 \end{aligned}$$

$$L_{\epsilon\tau G} = (c_1 - G\epsilon c_1)(c_2 + G\tau),$$

$$N_{e\tau G} = (c_1 + G\varepsilon)(c_2 - G\tau c_2),$$

$$D_{e\tau}(k) = q\tilde{q}B_\gamma(k) + g_e\tilde{g}_\tau B_Z(k),$$

$$|K_{e\tau G}| = -\{-c_\varepsilon(\varepsilon\tau + c_1c_2) + s_1s_2c_{\varphi_2} - s_\varepsilon(G\varepsilon c_2 + G\tau c_1)\}. \quad (17)$$

The above spin amplitudes are shorter than the corresponding formulae for the differential cross-section. Relations between spin amplitudes for bremsstrahlung from initial and final states as well as relations between  $Z_0$  and pure QED contributions are clearly visible.

It should be noted that in the case of soft photon limit these spin amplitudes seem not to coincide, as expected, with Born amplitudes multiplied by an infrared factor (e.g. they are complex and depend on photon circular polarization). This, however, stems out from the use of different parametrizations of the phase space in the soft and hard cross-sections and is of pure kinematical origin.

### 2.3.2. Photon spectrum

Due to simplicity of the hard bremsstrahlung spin amplitudes, in our parametrization of the phase space, the integrations over the angular variables may be performed explicitly and, as a result, I obtain the distribution of the photon energy  $d\sigma/dk$ . This result will be used as an important ingredient in the construction of the next M.C. program [5], therefore I shall present it here in this Section.

I start from the differential cross-section

$$d\sigma_{e\tau G}^{\mathcal{EF}} = |M_{e\tau G}^{\mathcal{EF}}|^2 d\text{Lips}_3 \quad (18)$$

and the result of integration over the angular variables reads as follows

$$\begin{aligned} d\sigma_{e\tau}^{++} &= \sigma_0 \left\{ 2 \frac{\alpha}{\pi} q^2 \frac{1-k}{k} \left[ \frac{1+(1-k)^2}{2} \left( \ln \left( \frac{S}{m_e^2} \right) - 1 \right) - \frac{k^2}{2} \right] |D_{e\tau}(k)|^2 \right. \\ &\quad + 2 \frac{\alpha}{\pi} \tilde{q}^2 \frac{1}{k} \left[ \frac{1+(1-k)^2}{2} \left( \ln \left( \frac{S}{\tilde{m}_\tau^2} \right) - 1 \right) - \frac{k^2}{2} \right] |D_{e\tau}(0)|^2 \\ &\quad \left. + 2 \frac{\alpha}{\pi} q\tilde{q}(-3\varepsilon\tau) \operatorname{Re} [D_{e\tau}(k)D_{e\tau}^*(0)] (1-k) \left( \frac{1}{k} - \frac{1}{2} \right) \right\} dk \\ d\sigma_{e\tau}^{-+} &= \sigma_0 \frac{\alpha}{\pi} q^2 \frac{k(1-k)}{2} [|D_{-e,\tau}(k)|^2 + |D_{e,\tau}(k)|^2] dk, \\ d\sigma_{e\tau}^{+-} &= \sigma_0 \frac{\alpha}{\pi} \tilde{q}^2 \frac{k}{2} [(D_{e,-\tau}(0)|^2 + |D_{e,\tau}(0)|^2] dk, \end{aligned} \quad (19)$$

where  $\sigma_0 = 4\alpha^2\pi/(3S)$ .

Note that the spin configurations which do not conserve helicity contribute to the integrated hard bremsstrahlung cross-section. Their contributions are smaller than those of the helicity conserving configurations, and they do not contain the infrared singularity

$1/k$ . In fact their contributions tend linearly to zero for small  $k$ . Furthermore, they do not contain leading logarithmic terms  $\ln(m_e^2/S)$ ,  $\ln(m_\tau^2/S)$ . That is why they may be neglected in the leading logarithm approximation, but should be kept as a contribution to corrections of order  $O(\alpha)$ .

### 2.3.3. Soft bremsstrahlung

Due to infrared singularity, contribution from soft real photon has to be integrated analytically and later combined with the virtual photon contribution. The soft photon cross-section is given by

$$(d\sigma_{e\tau}^{++})^{\text{SOFT PH}} = \left\{ |M_{e\tau}^{\text{BORN}}|^2 \delta^1 + \text{Re} \left[ (M_{e\tau}^{\text{BORN}})^* \left( -ie^2 \frac{c_e c_\tau}{S} \right) \right. \right. \\ \left. \left. (\varepsilon\tau + c) g_e \tilde{g}_\tau B_Z(0) \delta^2 + \left| -ie^2 \frac{c_e c_\tau}{S} \right|^2 ((\varepsilon\tau + c) g_e \tilde{g}_\tau)^2 |B_Z(0)|^2 \delta^3 \right] \right\} d\text{Lips}_2, \quad (20)$$

where

$$\delta^1 = q^2 \delta_S^1(m_e) + \tilde{q}^2 \delta_S^1(m_\tau) + \delta_{\text{int}}^1, \\ \delta_S^1(m) = -\frac{\alpha}{\pi} \left\{ \left[ 2 + 2 \ln \left( \frac{m^2}{S} \right) \right] \ln \left( \frac{2Ek_0}{\lambda} \right) + \ln \left( \frac{m^2}{S} \right) \right. \\ \left. + \frac{\pi^2}{3} + \frac{1}{2} \ln^2 \left( \frac{m^2}{S} \right) \right\}, \\ \delta_{\text{int}}^1 = \frac{\alpha}{\pi} q \tilde{q} \left\{ 4 \ln \left( \frac{1-c}{1+c} \right) \ln \left( \frac{2Ek_0}{\lambda} \right) + \ln^2 \left( \frac{1-c}{2} \right) \right. \\ \left. - \ln^2 \left( \frac{1+c}{2} \right) + 2 \text{Li}_2 \left( \frac{1+c}{2} \right) - 2 \text{Li}_2 \left( \frac{1-c}{2} \right) \right\}, \\ \delta^2 = \frac{4\alpha}{\pi} [\ln(\zeta + i\gamma) - \ln(\zeta - k_0 + i\gamma)] \\ \left\{ -q^2 \left( 1 + \ln \left( \frac{m_e^2}{S} \right) \right) + q \tilde{q} \ln \left( \frac{1-c}{1+c} \right) \right\}, \\ \delta^3 = \frac{2\alpha}{\pi} \left\{ q^2 \left[ -1 - \ln \left( \frac{m_e^2}{S} \right) \right] \frac{\zeta}{\gamma} \left[ \arctan \left( \frac{k_0 - \zeta}{\gamma} \right) \right. \right. \right. \\ \left. \left. - \arctan \left( -\frac{\zeta}{\gamma} \right) \right] + q^2 \left( 1 + \ln \left( \frac{m_e^2}{S} \right) \right) \right. \\ \left. \left[ \ln(\zeta + i\gamma) - \ln(\zeta - k_0 + i\gamma) \right] \right\}, \quad (21)$$

and  $k_0$  denotes upper limit on the photon energy to be considered as soft. The function  $\arctan(x)$  is defined in such a way that  $\arctan(\pm\infty) = \pm\pi/2$ .

Taking only dominant term  $\delta^1$  one can formally write spin amplitude for the soft bremsstrahlung as

$$(M_{\tau\tau}^{++})^{\text{SOFT PH}} = (M_{\tau\tau}^{++})^{\text{BORN}} \frac{1}{2} \delta^1. \quad (22)$$

Obviously this amplitude cancels out infrared singularity of virtual corrections.

It was checked that formula (20) reconstructs contribution of the soft photons as given in Ref. [19]. It was also checked numerically that formula (20) agrees well (at 1% accuracy level) with the approximate formula given in Refs [6, 7].

### 3. Chiral limit of density matrix formalism

Until now I discussed only spin amplitudes for the production of  $\tau$  pair and cross-sections in pure helicity states. In the practical applications, in order to calculate cross-sections, spin amplitudes have to be combined with density matrices of incoming  $e^\pm$  and with  $\tau^\pm$  decay. This point was elaborated in Refs [8, 15]. It was also extensively discussed in Chapter 2 of Ref. [11]. Since the density matrix of electron and positron mixes contributions of different helicity states, one cannot, in general, represent the cross-section as a non-coherent sum of cross-sections in different helicity configurations. Later in this Section it will be proven that it can be done so, when the following assumptions hold:

- I — polarization vectors of  $e^+$  and  $e^-$  are parallel to their momenta<sup>1</sup>.
- II — ultrarelativistic limit is taken i.e. terms  $m_e/E$ ,  $m_\tau/E$  are sufficiently small.

In general the differential cross-section for the process  $e^+e^- \rightarrow \tau^+\tau^-$ ,  $\tau^\pm \rightarrow X^\pm$  can be written as follows:

$$d\sigma = \sum_{KK'} \sum_{abcd} \tilde{e}_1^a \tilde{e}_2^b R_{abcd} (\tilde{\chi}_1^c)^K (\tilde{\chi}_2^d)^{K'} d\text{Lips}_2 d\tau_1^K d\tau_2^{K'}. \quad (23)$$

Here  $\tilde{e}_1^a = (1, \vec{e}_1)$ ,  $\tilde{e}_2^b = (1, \vec{e}_2)$  and  $\vec{e}_1, \vec{e}_2$  denote positron and electron polarization vectors in respectively  $RS_1(e^\pm)$  frames (see Fig. 1). Index  $K$  numbers various  $\tau$  decay channels. We will call  $\tilde{e}_{1,2}^a$  polarization four-vectors. The other four-vectors  $(\tilde{\chi}_{1,2}^c)^K$  are related to  $\tau^\pm$  decay product momenta. Differential cross-section of  $\tau^\pm$  (with polarization vector  $\tilde{\omega}_{1,2}$ ) decay in its  $RS(\tau^\pm)$  system reads

$$dp_{1,2} = \sum_K ((\tilde{\chi}^0)^K + \sum_{a=1}^3 \tilde{\omega}_a (\tilde{\chi}^a)^K) d\tau_{1,2}^K, \quad (24)$$

where  $d\tau_{1,2}^K$  denote elements of the  $\tau^\pm$  decay phase space in the decay channel  $K$ .

<sup>1</sup> This condition may be softened to a requirement of averaging observable quantities in the angle around the beam direction before comparing the results of calculations with the experimental data.

The procedure of averaging eliminates the effects of transverse polarization. This point was discussed in [22]. This proof holds only in the leading log limit. In general however, one gets contributions from the collinear hard photons which may not disappear from the cross-section in the  $m_{e,\tau} \rightarrow 0$  limit, even after averaging around beam direction.

Tensor  $R$  is related to spin amplitudes by means of contraction with Pauli matrices  $\sigma^i$ ,  $i = 1, 2, 3$  supplemented with  $\sigma^0 = I$ .

$$R_{abcd} = \frac{1}{8} \sum_{e, e', \bar{e}, \bar{e}'} \sum_{\tau, \tau', \bar{\tau}, \bar{\tau}'} \sigma_{e\bar{e}}^a \sigma_{e'\bar{e}'}^b (M_{e, \tau}^{e\bar{e}', \tau\tau'}) (M_{\bar{e}, \bar{\tau}}^{e\bar{e}', \tau\tau'})^* \sigma_{\tau\bar{\tau}}^c \sigma_{\tau'\bar{\tau}'}^d. \quad (25)$$

In the case of the hard bremsstrahlung additional summation over photon polarization is included implicitly in the definition of tensor  $R$ . In the simple case of one prong decay, when only one charged particle is observed,  $(\chi^i)^K$ ,  $i = 1, 2, 3$  forms a vector proportional to momentum of the charged decay product<sup>2</sup> [23, 24]. In this case it is possible to average partially the decay distribution over the angle around  $\tau^\pm$  direction. This leads to significant simplification of the formula (23). The sum over the indices  $a, b, c, d = 0, 1, 2, 3$  reduces only to 0 and 3. One is left with only 16 elements of the tensor  $R$ .

Let us express polarization four-vectors  $\tilde{e}_1^a$  and  $\tilde{e}_2^b$  as a linear combination of the polarization four-vectors of pure helicity states (pure in the quantum mechanical sense)  $\tilde{e}_\pm^a$ .

$$\tilde{e}_\pm^a = (1, 0, 0, \pm 1), \quad \tilde{e}_{1,2}^a = p_{1,2}^+ \tilde{e}_+^a + p_{1,2}^- \tilde{e}_-^a, \quad (26)$$

where  $p_{1,2}^\pm$  are interpreted as a probabilities of finding right/left handed  $e^+$  and left/right  $e^-$  in the beams.

The same can be done with the four-vectors  $\tilde{\chi}_1^a$  and  $\tilde{\chi}_2^b$ . They can be also represented as a linear combination of  $\tilde{e}^\pm$ .

$$(\tilde{\chi}_{1,2}^a)^K = a_{1,2}^K [(q_{1,2}^+)^K (\tilde{e}^+)^a + (q_{1,2}^-)^K (\tilde{e}^-)^a]. \quad (27)$$

Now, by contracting  $(\tilde{e}^\pm)^a$  vectors with tensor  $R$  and using its definition (25) the formula (23) may be rewritten as follows

$$d\sigma = \sum_{e\tau e'\bar{\tau}} p_1^e p_2^{e'} |M_{e\tau}^{e\bar{e}'}|^2 d\text{Lips}_2 \left( \sum_K a_1^K (q_1^\tau)^K d\tau_1^K \right) \left( \sum_{K'} a_2^{K'} (q_2^{\bar{\tau}})^{K'} d\tau_2^{K'} \right), \quad (28)$$

where  $\sum_K a_{1,2}^K (q_{1,2}^\tau)^K d\tau_{1,2}^K$  represents the differential cross-section for the decay of  $\tau^\pm$  in the pure helicity states.

The above shows that differential cross-section for production of  $\tau^\pm$  pair can be generated in a M.C. program as an incoherent sum of cross-sections for various helicity configurations of  $e^+$ ,  $e^-$ ,  $\tau^-$ ,  $\tau^+$ . Therefore in the M.C. procedure longitudinal spin polarization may be implemented in the following way: first  $e^\pm$  and  $\tau^\pm$  helicities are chosen randomly according to integrated cross-section. Then  $\tau$  production and decay is simulated as if  $e^\pm$  and  $\tau^\pm$  were 100% polarized according to the chosen helicities. Note that this procedure, which is generally not valid due to general quantum mechanical principles [25], is applicable here due to our assumptions I-II.

<sup>2</sup> In the case of multiprong decay this three vector is a combination of the momenta of the decay products.

#### 4. Simplified Monte Carlo for $e^+e^- \rightarrow \tau^+\tau^-(\gamma)$

The formulae presented in Section 2 will be useful in constructing a M.C. program [5] dedicated specifically to the  $\tau^\pm$  production and decay process in the framework of GSW/QED, up to a very high accuracy. In this Section, however, I shall present an alternative M.C. algorithm which was used to obtain numerical results presented in the next Sections. These calculations are of the intermediate precision level ( $\sim 1\%$ ) because they do not include contributions of  $O((\alpha/\pi \ln(S/m_e^2))^2)$  and some of  $O(\alpha/\pi)$  (notably some genuine GSW terms), but they may be performed more easily and also earlier using a modification of the existing M.C. program for  $e^+e^- \rightarrow \mu^+\mu^-(\gamma)$  [7]. The two processes,  $\mu^\pm$  and  $\tau^\pm$  production, are physically quite similar (identical coupling to  $Z_0$  etc.) and furthermore  $4m_\tau^2/S$  for  $S \sim M^2$  is quite small. The only problem is that M.C. program of Ref. [7] does not include  $\tau^\pm$  polarizations which, as was shown in the previous Section, are necessary even in the  $m_\tau \rightarrow 0$  limit (helicity conservation).

In the following we shall show how to do a modifications of the existing analytical calculations for  $e^+e^- \rightarrow \mu^+\mu^-(\gamma)$ , and the corresponding M.C. program, in order to include spin polarizations.

Since  $e^-$  will be polarized in SLC experiment I shall also include  $e^\pm$  longitudinal polarizations in the presented formulae.

Let us start with the following observation: if one works out the Born cross-section for the reaction  $e^+e^- \rightarrow \tau^+\tau^-$  in the  $Z_0$  region with the classical techniques with traces over strings of Dirac matrices then it can be generally written in the following way:

$$\begin{aligned}
 d\sigma \sim & \left\{ \text{Tr} [\gamma^\mu (\not{p}_1 - m_e) (1 + \gamma_5 \not{\epsilon}_1) \gamma^\nu (\not{p}_2 + m_e) (1 + \gamma_5 \not{\epsilon}_2)] \right. \\
 & \times \text{Tr} [\gamma_\mu (\not{q}_1 - m_\tau) (1 + \gamma_5 \not{\tilde{\epsilon}}_1) \gamma_\nu (\not{q}_2 + m_\tau) (1 + \gamma_5 \not{\tilde{\epsilon}}_2)] + 2 \text{Re} \frac{1}{B_Z(0)} \\
 & \times \text{Tr} [(v\gamma^\mu + a\gamma_5\gamma^\mu) (\not{p}_1 - m_e) (1 + \gamma_5 \not{\epsilon}_1) \gamma^\nu (\not{p}_2 + m_e) (1 + \gamma_5 \not{\epsilon}_2)] \\
 & \times \text{Tr} [(\tilde{v}\gamma_\mu + \tilde{a}\gamma_5\gamma_\mu) (\not{q}_1 - m_\tau) (1 + \gamma_5 \not{\tilde{\epsilon}}_1) \gamma_\nu (\not{q}_2 + m_\tau) (1 + \gamma_5 \not{\tilde{\epsilon}}_2)] + \frac{1}{|B_Z(0)|^2} \\
 & \times \text{Tr} [(v\gamma^\mu + a\gamma_5\gamma^\mu) (\not{p}_1 - m_e) (1 + \gamma_5 \not{\epsilon}_1) (v\gamma^\nu + a\gamma^\nu) (\not{p}_2 + m_e) (1 + \gamma_5 \not{\epsilon}_2)] \\
 & \left. \times \text{Tr} [(\tilde{v}\gamma_\mu + \tilde{a}\gamma_5\gamma_\mu) (\not{q}_1 - m_\tau) (1 + \gamma_5 \not{\tilde{\epsilon}}_1) (\tilde{v}\gamma_\nu + \tilde{a}\gamma_\nu) (\not{q}_2 + m_\tau) (1 + \gamma_5 \not{\tilde{\epsilon}}_2)] \right\} d \text{Lips}_2. \quad (29)
 \end{aligned}$$

Here  $\omega_1, \omega_2, \tilde{\omega}_1, \tilde{\omega}_2$  denote polarization vectors of  $e^+, e^-, \tau^+, \tau^-$ ,  $\tilde{\omega}_{1,2}^2 = \omega_{1,2}^2 = -1$ . Now, in the chiral limit this formula can be rewritten in the following way:

$$d\sigma \sim \left\{ \text{Tr} [\gamma^\mu \not{p}_1 (1 + \epsilon\gamma_5) \gamma^\nu \not{p}_2 (1 + \epsilon'\gamma_5)] \text{Tr} [\gamma_\mu \not{q}_1 (1 + \tau\gamma_5) \gamma_\nu \not{q}_2 (1 + \tau'\gamma_5)] \right\}$$

$$\begin{aligned}
& + 2 \operatorname{Re} \frac{1}{B_Z(0)} \operatorname{Tr} [(v\gamma^\mu + a\gamma_5\gamma^\mu) \not{P}_1 (1 + \varepsilon\gamma_5) \gamma^\nu \not{P}_2 (1 + \varepsilon'\gamma_5)] \\
& \quad \operatorname{Tr} [(\tilde{v}\gamma_\mu + \tilde{a}\gamma_5\gamma_\mu) \not{Q}_1 (1 + \tau\gamma_5) \gamma_\nu \not{Q}_2 (1 + \tau'\gamma_5)] \\
& + \frac{1}{|B_Z(0)|^2} \operatorname{Tr} [(v\gamma^\mu + a\gamma_5\gamma^\mu) \not{P}_1 (1 + \varepsilon\gamma_5) (v\gamma^\nu + a\gamma_5\gamma^\nu) \not{P}_2 (1 + \varepsilon'\gamma_5)] \\
& \quad \operatorname{Tr} [(\tilde{v}\gamma_\mu + \tilde{a}\gamma_5\gamma_\mu) \not{Q}_1 (1 + \tau\gamma_5) (\tilde{v}\gamma_\nu + \tilde{a}\gamma_5\gamma_\nu) \not{Q}_2 (1 + \tau'\gamma_5)] \Big\} d \operatorname{Lips}_2. \quad (30)
\end{aligned}$$

Here  $\varepsilon$ ,  $-\varepsilon'$ ,  $\tau$ ,  $-\tau'$  denote helicities of  $e^+$ ,  $e^-$ ,  $\tau^+$ ,  $\tau^-$ , respectively. By means of collecting all  $\gamma_5$  matrices together formula (30) can be rewritten as follows

$$\begin{aligned}
d\sigma \sim & \left\{ \operatorname{Tr} [\gamma^\mu \not{P}_1 \gamma^\nu \not{P}_2] \operatorname{Tr} [\gamma_\mu \not{Q}_1 \gamma_\nu \not{Q}_2] \left( c_0 + \operatorname{Re} \frac{1}{B_Z(0)} c_1 + \frac{1}{|B_Z(0)|^2} c_2 \right) \right. \\
& \left. + \frac{1}{2} \operatorname{Tr} [\gamma_5 \gamma^\mu \not{P}_1 \gamma^\nu \not{P}_2] \operatorname{Tr} [\gamma_5 \gamma_\mu \not{Q}_1 \gamma_\nu \not{Q}_2] \left( d_0 + \operatorname{Re} \frac{1}{B_Z(0)} d_1 + \frac{1}{|B_Z(0)|^2} d_2 \right) \right\} d \operatorname{Lips}_2, \quad (31)
\end{aligned}$$

where

$$\begin{aligned}
c_0 &= (1 + \varepsilon\varepsilon') (1 + \tau\tau'), \\
c_1 &= 2[v(1 + \varepsilon\varepsilon')\tilde{v}(1 + \tau\tau') + a\tilde{a}(\varepsilon + \varepsilon')(\tau + \tau')], \\
c_2 &= [(a^2 + v^2)(1 + \varepsilon\varepsilon') + 2va(\varepsilon + \varepsilon')] [(\tilde{v}^2 + \tilde{a}^2)(1 + \tau\tau') + 2\tilde{v}\tilde{a}(\tau + \tau')], \\
d_0 &= 2(\varepsilon + \varepsilon')(\tau + \tau'), \\
d_1 &= 4[a\tilde{a}(1 + \varepsilon\varepsilon')(1 + \tau\tau') + v\tilde{v}(\varepsilon + \varepsilon')(\tau + \tau')], \\
d_2 &= 2[2va(1 + \varepsilon\varepsilon') + (v^2 + a^2)(\varepsilon + \varepsilon')] [2\tilde{v}\tilde{a}(1 + \tau\tau') + (\tilde{v}^2 + \tilde{a}^2)(\tau + \tau')]. \quad (32)
\end{aligned}$$

In these expressions one finds again familiar terms  $c_0$ ,  $c_1$ ,  $c_2$ ,  $d_0$ ,  $d_1$ ,  $d_2$  which were used in the program [7]. As a result the  $\tau^\pm$  differential cross-section has the same structure, only factors  $c_0$ ,  $c_1$ ,  $c_2$ ,  $d_0$ ,  $d_1$ ,  $d_2$  are now dependent on fermions' helicities.

This result applies to a whole soft part of the cross-section. Things get more complicated in the case of the hard bremsstrahlung. The set of coefficients (32) has to be extended.

$$\begin{aligned}
c_3 &= [v(1 + \varepsilon\varepsilon') + a(\varepsilon + \varepsilon')] [\tilde{a}(1 + \tau\tau') + \tilde{v}(\tau + \tau')] \\
& \quad - [a(1 + \varepsilon\varepsilon') + v(\varepsilon + \varepsilon')] [\tilde{v}(1 + \tau\tau') + \tilde{a}(\tau + \tau')], \\
d_3 &= [v(1 + \varepsilon\varepsilon') + a(\varepsilon + \varepsilon')] [\tilde{a}(1 + \tau\tau') + \tilde{v}(\tau + \tau')] \\
& \quad + [a(1 + \varepsilon\varepsilon') + v(\varepsilon + \varepsilon')] [\tilde{v}(1 + \tau\tau') + \tilde{a}(\tau + \tau')],
\end{aligned}$$

$$\begin{aligned}
c_4 = & \frac{1}{2} [(v^2 + a^2)(1 + \varepsilon\varepsilon') + 2va(\varepsilon + \varepsilon')] [(\tilde{v}^2 + \tilde{a}^2)(\tau + \tau') + 2\tilde{v}\tilde{a}(1 + \tau\tau')] \\
& - \frac{1}{2} [(v^2 + a^2)(\varepsilon + \varepsilon') + 2va(1 + \varepsilon\varepsilon')] [(\tilde{v}^2 + \tilde{a}^2)(1 + \tau\tau') + 2\tilde{v}\tilde{a}(\tau + \tau')], \\
d_4 = & \frac{1}{2} [(v^2 + a^2)(1 + \varepsilon\varepsilon') + 2va(\varepsilon + \varepsilon')] [(\tilde{v}^2 + \tilde{a}^2)(\tau + \tau') + 2\tilde{v}\tilde{a}(1 + \tau\tau')] \\
& + \frac{1}{2} [(v^2 + a^2)(\varepsilon + \varepsilon') + 2va(1 + \varepsilon\varepsilon')] [(\tilde{v}^2 + \tilde{a}^2)(1 + \tau\tau') + 2\tilde{v}\tilde{a}(\tau + \tau')]. \quad (33)
\end{aligned}$$

I get also, for helicity nonconserving configurations, the contributions to the cross-section which cannot be directly represented in the language of coefficients  $c_0, c_1, \dots$ . But because these residual contributions from helicity nonconserving configurations, as pointed out in Section 2.3.2, are small (1 %). I shall omit them for a moment. Neglecting above contributions the whole spin dependence of the cross-section may be confined to the coefficients  $c_0, c_1, c_2, c_3, c_4, d_0, d_1, d_2, d_3, d_4$ .

Thus in order to simulate the  $\tau$  pair production process I may use an old muon program [7] provided the appropriate redefinition of coefficients  $c_i, d_i$  is made.

### 5. Radiative corrections of the GSW model

A number of independent groups [26–33] have calculated one loop  $O(\alpha)$  GSW radiative corrections to the lepton/quark interactions. The calculations may differ in the choice of the renormalization scheme and in the choice of the input experimental data, but generally the tendency is to use on-shell renormalization schemes because they can accommodate classical QED bremsstrahlung calculations in almost unchanged form and the experimental data on mass of  $Z_0$  and  $W^\pm$  may be used directly as the input data. Furthermore, some large logarithms coming from trivial corrections of the vacuum polarization type may be easily located and hidden in the lowest order (or input) parameters like  $M, \alpha, G_F, M_W$ .

In the numerical calculations presented later in this work we aim at keeping  $O(\alpha/\pi \ln(S/m_e^2))$  terms and some  $O(\alpha/\pi)$  terms (with respect to lowest order). The trivial large logarithms effects are however taken into account by including vacuum polarization corrections to the  $\gamma$  and  $Z_0$  propagators and using a proper definition of  $M$  and  $\sin^2 \theta_W$ . The remaining GSW effects are then of  $O(\alpha/\pi)$  and are numerically rather small. I postpone their inclusion to the forthcoming work [5].

In practical terms, I have made the following modification of the  $Z_0$  propagator both in the soft and hard bremsstrahlung part of the M.C. program:

$$Z(S) = \frac{1}{S - M^2 + i\Gamma M} \rightarrow \frac{1}{S - M^2 + \Pi_T^{ZZ}(S)}, \quad (34)$$

where  $\Pi_T^{ZZ}(S)$  is defined in Ref. [27], formula (2.2.30).

The effects due to above modifications are added during the final rejection procedure in the M.C. algorithm. This rejection was already present in the program of Ref. [7] and its purpose was the introduction of some interference terms. The efficiency of the program is not diminished by this modification.

The initial parameters in the program are appropriately redefined.  $Z_0$  mass  $M$  is treated



as an input parameter and coupling constants are calculated again in terms of  $\sin^2 \theta_w$ , but now with  $\sin^2 \theta_w = 1 - M_w^2/M^2$ . Since  $W^\pm$  mass  $M_w$  is not known precisely enough, it is, therefore, calculated using  $M$  and muon life time, from formula (3.1.4) of Ref. [27]. The width of  $Z_0$  is the necessary input parameter of the program and it is taken as  $\Gamma = \text{Im}(\Pi_T^{ZZ}(M^2))/M$ . This  $\Gamma$  plays only the rôle of a dummy parameter in the generation of the raw events, prior to final rejection. The final rejection introduces  $\Pi_T^{ZZ}$  in  $Z_0$  propagator with full  $S$  dependence both in the real and imaginary parts. The photon vacuum polarization  $\Pi_{\gamma\gamma}(S)$  in the program is also replaced with  $\Pi_T^{AA}(S)$  of Ref. [27]. For  $\sqrt{S} \lesssim 10$  GeV,  $\Pi_T^{AA}(S)$  is corrected to be compatible with the results based on the dispersion relations approach [16, 17, 18].

The above procedure introduces the most important GSW effects. The contributions which are still left out, are of  $O(\alpha)$  i.e. numerically rather small, but should be included in the future version of the M.C. program, aiming at a higher precision level.

## 6. Numerical results

In this Section I present some numerical results obtained using the M.C. program described in Section 4. They mainly concern the measurement of the  $\tau$  polarization in the  $Z_0$  region.

The following input parameters were used in the calculations:  $M = 93$  GeV,  $m_{\text{top}} = 30$  GeV,  $m_{\text{HIGGS}} = 100$  GeV. The mass of the  $W$  boson  $M_w = 82.02$  GeV, was calculated out of  $M$  and the muon life-time. This yields  $\sin^2 \theta_w = 1 - (M_w/M)^2 = 0.222$ . The width of  $Z_0$  was found to be  $\Gamma = 2.56$  GeV.

Before some specific results are shown, let us recapitulate some basic properties of the corrections due to QED bremsstrahlung. One may expect that since the leading logarithm expansion parameter  $\alpha/\pi \ln(S/m_e^2) \sim 0.06$ , the radiative effect should not be much higher than just 6%. The examples of the total cross-section and muon asymmetry in Ref. [6, 7] demonstrates however that such corrections may be well above 100%.

These large effects are related to the events with hard collinear bremsstrahlung out of  $e^\pm$  beams. Quite fortunately they are usually rather easy to remove from the data by applying standard cut-offs like maximum acollinearity and minimum energy.

It is perhaps worth mentioning that the above kinematical amplification of the radiative effects takes place for quantities which are strongly varying when  $S(S > M^2)$  gets reduced (due to initial state bremsstrahlung) to  $S = M^2$ . This effect is weak on the top of  $Z_0$ .

In the presented results I shall try to eliminate the above trivial kinematical effect wherever it is possible by means of suitable kinematical cut-off's (like in the experiment).

In Figs 2 and 3 I examine the influence of the radiative corrections on the  $\tau^-$  polarization in the  $e^+e^- \rightarrow \tau^+\tau^-(\gamma)$  process. The  $\tau^-$  polarization is, of course, not a directly measurable quantity but I show these plots in order to get an idea about radiative corrections to  $\tau^-$  spin polarization, neglecting (for the moment) problems related to its measurement. In order to get rid of the effects related to hard initial state bremsstrahlung (especially for  $S > M^2$ ) we employed the cut-off  $E_\gamma/E > 0.2$  on the photon energy. Such a cut-off cannot be realized in the experiment directly because the photon momentum is lost in the beam

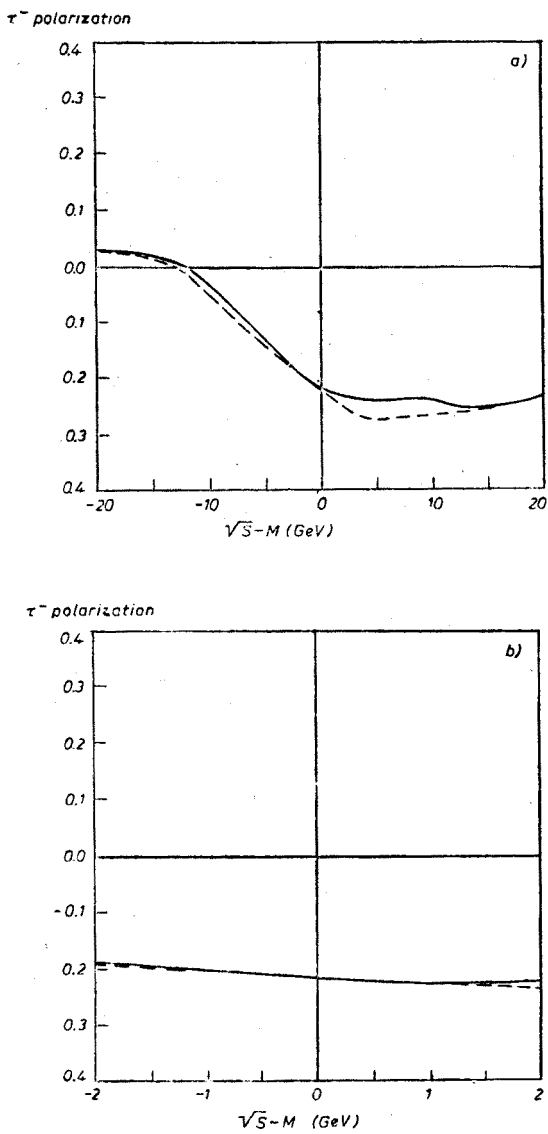


Fig. 2.  $\tau^-$  polarization as a function of the CMS energy. The solid line corresponds to the cross-section with radiative corrections; the dashed one to lowest order (no beam polarization). Figs 2a, 2b correspond to different energy scale. Cut off  $E_\gamma/E < 0.2$ . The average over  $4\pi$  angle is taken

pipe (in most cases) and  $\tau^-$  momenta are not measured directly. Nevertheless this cut-off corresponds roughly to some more complicated set of cut-offs defined later in this Section using momenta of charged decay products.

In Fig. 2, the  $\tau^-$  polarization is plotted as a function of  $\sqrt{S}-M$ , with and without radiative corrections, taking unpolarized  $e^\pm$  beams. As we see the radiative corrections are of order  $-4-12\%$  and are larger for  $S > M^2$ . It should be noted that  $\tau^-$  polarization

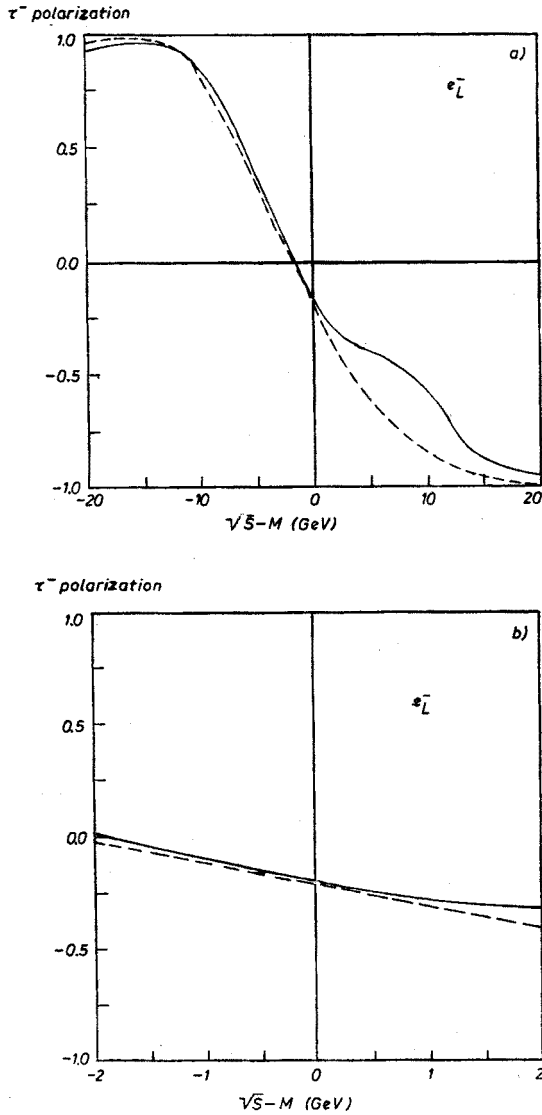


Fig. 3.  $\tau^-$  polarization as a function of the CMS energy. The solid line corresponds to the cross-section with radiative corrections; the dashed one to lowest order (pure left handed electron beam). Figs 3a, b correspond to different energy scale. Cut off  $E_\gamma/E < 0.2$ . The average over  $4\pi$  angle is taken

for unpolarized  $e^\pm$  depends weakly on  $S$  in  $S > M^2$  region and therefore it is not prone to the problems due to initial state bremsstrahlung.

This is less the case for the  $\tau^-$  polarization when beams are polarized. In Fig. 3 the similar, as in Fig. 2, plot is presented for left-handedly polarized  $e^-$  (and  $e^+$  unpolarized). Since in this case  $\tau^-$  polarization depends rather strongly on  $S$  for  $S > M^2$ , we observe that radiative corrections are bigger in this region of  $S$  than in Fig. 2 and are of order of

40%. This sizeable effect would have extended to much higher CMS energies if my cut-off on photon energy were less restrictive. In Figs 2 and 3 the  $\tau^-$  polarization was averaged over the  $\tau^-$  angular distribution.

For a right handed electron beam polarization one obtains a plot analogous to Fig. 3 but with the reversed sign of the  $\tau^-$  polarization.

In Figs 4 and 5 I show some distributions which are also related to  $\tau$  polarization, but are directly measurable in the experiments, using  $\tau^+$  decay products.

Fig. 4 shows the energy distribution of  $\pi^+$  (normalized to the unity) originating from  $\tau^+$  decay. The other side  $\tau^-$  is assumed to decay into one prong channel ( $\pi^- \nu, \rho^- \nu, e^- \bar{\nu}, \mu^- \bar{\nu}$ ). The production process  $e^+e^- \rightarrow \tau^+\tau^-(\gamma)$  is taken here at  $S = M^2$  and only rather mild cut-offs are employed:  $\xi = \angle(\vec{p}_+, \vec{p}_-) < 45^\circ$ ,  $|\vec{p}_+| > 1 \text{ GeV}$ ,  $|\vec{p}_-| > 1 \text{ GeV}$  and  $\theta_\pm > 15^\circ$ , where  $\vec{p}_\pm$  are momenta of the charged  $\tau^\pm$  decay products and  $\theta_\pm$  is the angular distance of  $p_\pm$  from the beam pipe. As it may be seen in Fig. 4 the radiative corrections for  $\tau$  polarization measurement the top of  $Z_0$  peak, for unpolarized  $e^-$  are rather small, of order of 5% but are significantly bigger than for  $\tau$  polarization itself.

In Fig. 5 the same distribution is shown for left handed  $e^-$  and for  $S = M + 10 \text{ GeV}$ . Here, since we expect strong effects due to initial state bremsstrahlung we employ more stringent cut-offs  $\xi < 20^\circ$ ,  $|\vec{p}_\pm| > 5 \text{ GeV}$ ,  $\theta_\pm < 15^\circ$  which correspond roughly to  $E_\gamma/E < 0.3$  (as was checked by inspection of the corresponding photon energy distribution). In this case even more restrictive cut-offs cannot eliminate influence of the initial state bremsstrahlung. Radiative corrections are bigger than in Fig. 4 and are of order of 25%. Also, the distribution departs from the linear shape due to radiative corrections and cut-offs. The above effect in the case of the left handed electron beam is even larger.

Having in hand a M.C. program it is easy to calculate many other cross-sections and distributions for the simulated process. I conclude my presentation of the numerical

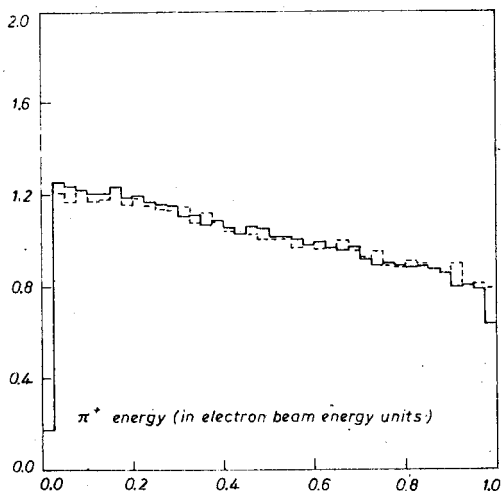


Fig. 4. Energy distribution of  $\pi^+$  from the  $\tau^+$  decay for CMS energy of  $Z_0$  mass. Solid line corresponds to the cross-section with radiative corrections, dashed one to the lowest order (no beam polarization). Cut-offs (defined in the text) were included

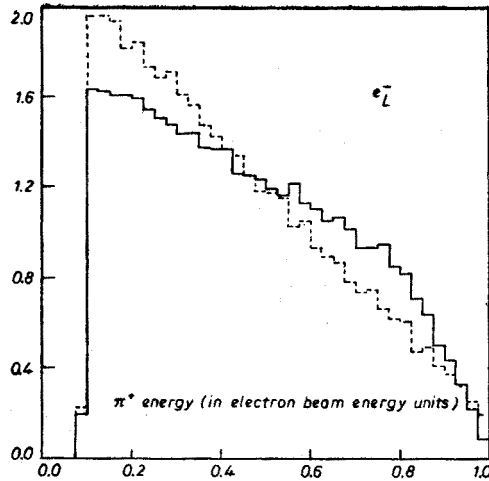


Fig. 5. Energy distribution of  $\pi^+$  from the  $\tau^+$  decay for CMS energy 10 GeV above  $Z_0$  mass. Solid line corresponds to the cross-section with radiative corrections, dashed one to the lowest order (left handed electron beam). Cut-offs (defined in the text) were included

results here, with the following remark. As it is seen from Figs 2 and 4, the influence of the QED bremsstrahlung on the measurement of  $\tau$  polarization on the top of  $Z_0$  is not very strong ( $\sim 4\%$ ) and therefore it does not decrease the quality of this observable as a good candidate for a data point in the precise tests of GSW electroweak theory. The influence of the QED bremsstrahlung on the  $\tau$  polarization off  $Z_0$  peak will be stronger and more difficult to eliminate.

## 7. Summary

The  $\tau$  production process has a number of characteristic features which, on one hand, make it very interesting (for the purpose of the precise tests of GSW theory) but, on the other hand, they create some technical problems.

In this paper I show how some of these problems, mainly connected to the spin structure of the process (in the presence of the QED bremsstrahlung) may be properly handled and solved.

In the first part of the work I calculate spin amplitudes for the production process and I calculate also some important distributions relevant for the construction of the Monte Carlo algorithm.

The following effects are included in these calculations:

1.  $Z_0$  exchange in the resonance form.
2. QED/GSW  $O(1\%)$  radiative corrections together with single bremsstrahlung from electron beams and final state  $\tau$ .
3. Longitudinal spin polarization for the initial and final state fermions.
4. Mass effects.

In the second part of the paper, I show how to connect generation and decay parts of the  $\tau$  production process, all the time having in mind the construction of the M.C. algorithm. In particular, I discuss in detail how one may take advantage of the fact that the  $\tau$  mass is relatively small (compared to  $Z_0$  mass) i.e. I discuss the question how to take properly chiral limit, not loosing or deforming spin effects in the final results. Here in solving properly these problems, the results from the first part of the work were rather helpful.

In the last part of the paper I present some numerical results which were obtained using the M.C. program based on the existing program for muon production and some ideas developed earlier in the paper. In the calculations all effects 1–4 listed above are included. Spin effects are introduced in the chiral limit. Missing are still some numerically small but finite mass effects, and some (also numerically small) one loop GSW radiative corrections.

Having at hand a M.C. program it is rather easy to produce a multitude of distributions, cross-sections asymmetries etc. I concentrate on such numerical results which would show how important (numerically) are radiative effects on the measurable quantities related to spin polarization of the  $\tau$ .

As expected the most drastic radiative effects due to initial state bremsstrahlung can be usually eliminated using an appropriate cut-offs. The strength of the remaining effects depends on the center of mass system energy (on the distance from the top of  $Z_0$  resonance), on the strength of the cut-offs, on the beam polarization and other factors. In the presented examples corrections vary from 2% to 40%.

Generally it seems however, that these effects can be brought under control, and it is unlikely that they could prevent the use of the  $\tau$  polarization as a probe for precise tests of the GSW theory.

The author is grateful to Prof. A. Białas for initial encouragement to start this investigation, to Dr. S. Jadach for invaluable guidance and cooperation in many stages of this work and to Prof. A. Kotański for help in preparing the final version of this paper. Very warm hospitality of the Centre de Physique des Particules de Marseille, where this work was completed, and helpful discussions with Prof. J. J. Aubert and members of Marseille Particle Physics Group (especially Dr. E. Kajfasz) are also acknowledged. I thank W. Kubicza for making available an IBM XT for part of numerical calculations.

#### REFERENCES

- [1] S. L. Glashow, *Nucl. Phys.* **22**, 579 (1961); S. Weinberg, *Phys. Rev. Lett.* **19**, 1264 (1967); A. Salam, Proc. of 8-th Nobel Symposium 1968, ed: N. Svartholm, Wiley 1968, p. 367; S. L. Glashow, J. Iliopoulos, L. Maiani, *Phys. Rev.* **D12**, 1285 (1970).
- [2] SLD Design report, SLAC-273, May 1984; SLC Report, SLAC-247, March 1982.
- [3] LEP Report, CERN-79-01, February 1979.
- [4] G. Altarelli, Physics at LEP, CERN 86-02, February 1986, p. 1.
- [5] S. Jadach, R. G. Stuart, Z. Wąs, in preparation.
- [6] F. A. Berends, R. Kleiss, S. Jadach, *Nucl. Phys.* **B202**, 63 (1982).
- [7] F. A. Berends, R. Kleiss, S. Jadach, *Comput. Phys. Commun.* **29**, 185 (1983).
- [8] S. Jadach, Z. Wąs, *Acta Phys. Pol.* **B15**, 1151 (1984).

- [9] R. Kleiss, *Nucl. Phys.* **B241**, 145 (1984); F. A. Berends, P. H. Daverveldt, R. Kleiss, *Nucl. Phys.* **B253**, 441 (1985).
- [10] F. A. Berends, P. De Causmaecker, R. Gastmans, R. Kleiss, W. Troost, Tai Tsun Wu, *Nucl. Phys.* **B264**, 243 (1986).
- [11] S. Jadach, *Acta Phys. Pol.* **B16**, 1007 (1985).
- [12] F. A. Berends, R. Kleiss, S. Jadach, Z. Wąs, *Acta Phys. Pol.* **B14**, 413 (1983).
- [13] J. D. Bjorken, S. D. Drell, *Relativistic Quantum Mechanics*, Mc Graw-Hill, New York 1964.
- [14] Z. Wąs, *Acta Phys. Austr. Suppl.* **XXVI**, 447 (1984).
- [15] S. Jadach, Z. Wąs, *Comput. Phys. Commun.* **36**, 191 (1985).
- [16] H. Burkhard, TASSO note no. 192, December 1981.
- [17] B. W. Lynn, G. Penso, C. Verzegnassi, *Phys. Rev.* **D35**, 42 (1987).
- [18] E. A. Paschos, *Nucl. Phys.* **B159**, 285 (1979).
- [19] M. Böhm, W. Hollik, *Nucl. Phys.* **B204**, 45 (1982).
- [20] R. W. Brown, R. Decker, E. A. Paschos, *Phys. Rev. Lett.* **52**, 1192 (1984).
- [21] F. A. Berends, R. Kleiss, P. De Causmaecker, R. Gastmans, W. Troost, *Nucl. Phys.* **B206**, 61 (1982).
- [22] K. Hikasa, *Phys. Lett.* **B143**, 266 (1984).
- [23] H. Kuhn, F. Wagner, *Nucl. Phys.* **B236**, 16 (1984).
- [24] J. Brau, G. J. Tarnopolsky, Spin momentum correlations in the decay  $\tau \rightarrow \rho \nu$ , SLC Workshop Notes CN-17, 1981.
- [25] *Quantum Theory and Measurement*, ed. J. A. Wheeler, W. Zurek, Princeton University Press 1983, Chapter 3.
- [26] B. W. Lynn, R. G. Stuart, *Nucl. Phys.* **B253**, 216 (1985).
- [27] R. G. Stuart, Radiative corrections to  $e^+e^- \rightarrow \mu^+\mu^-$  in the Glashow-Weinberg-Salam model, Rutherford Appleton Lab. preprint, RAL T008, Oxford 1985.
- [28] M. Böhm, W. Hollik, *Phys. Lett.* **139B**, 213 (1984).
- [29] W. Wetzel, *Nucl. Phys.* **B227**, 1 (1983).
- [30] A. Sirlin, *Phys. Rev.* **D22**, 971 (1980); W. J. Marciano, A. Sirlin, *Phys. Rev.* **D22**, 2695 (1980); S. Sarantakos, A. Sirlin, W. J. Marciano, *Nucl. Phys.* **B217**, 84 (1983).
- [31] S. Sakakibara, *Phys. Rev.* **D24**, 1149 (1981).
- [32] D. Yu. Bardin, V. A. Dokuchajeva, *Nucl. Phys.* **B246**, 221 (1984).
- [33] K. Aoki, Z. Hioki, R. Kawabe, M. Konuma, T. Muta, *Progr. Theor. Phys.* **65**, 1001 (1981).